

# ANGULAR DISTRIBUTION OF CERAMIC ISOLATOR SPUTTERED MATERIAL IN THE SPT JET

S.A.Khartov\*, V.K.Egorov\*\*, A.B.Nadiradze\*, Yu.V.Zikeeva\*

\* Moscow Aviation Institute (State Technical University) MAI  
Electric Propulsion and Space Power Plants Department  
4, Volokolamskoe sh., Moscow, 125971, Russia, [k208@mai.ru](mailto:k208@mai.ru)  
\*\* IPMT RAS, Chernogolovka, Moscow Region, Russia

*Method and measurement of angular distribution of sputtered material in the SPT jet are represented in the paper. The method of measurement bases on the idea of particles accumulation in the metallic film deposited onto a sample surface placed into the jet. The flow value was determined using boron concentration in the film (deposition time 12 hours). In order to exclude film sputtering by jet ions, samples were placed in trap's focus, which was done in the form of pyramid. The geometrical sizes of pyramid were selected in such a way that particle flow onto samples was equal to sputtered particles flow. As a result of the experiment the values of boron flows in the range of divergence angles 60 – 65 degrees was obtained (the flow value was  $\sim 10^{-12}$  1/cm<sup>2</sup>sec). The research was sponsored by CNRS.*

## Introduction

As it is known [1] in the ERT jet there is a few (up to 1-2%) admixture of sputtered isolator material besides the main plasma component. Under certain conditions such particles can be deposited on the SC surfaces changing their properties. Therefore in order to secure the reliability of the ERT and the SC joint operation it is necessary have information about sputtered particles flows in plasma jet of the ERT.

Needed information can be obtained from direct experiments. Solving such problem in [1] the solid-body targets were used (targets were placed in the ERT jet for a long time). In this case deposited flows were determined according to target mass or thickness change. But as far as not only particles of admixture are deposited on to the target's surface, but also sputtered material from the vacuum chamber walls, it is very difficult to determine sputtered products composition and angular distribution. Besides, simultaneously the two phenomenons are taken place: the film growth and sputtering with jet ions, so the additional error of measurement is happened.

In the works [2,3] in order to measure values and impurity particle composition a method of impurity particles "packing" in a metal layer deposited on the substrate was proposed. This method permits to reduce sufficiently an effect of repeated sputtering and to fixed non-condensing sputtering products (oxygen and nitrogen). But this method does not permit to exclude completely impurity particles sputtering.

## Experimental procedure

The scheme of the experiment and visual appearance of the test facility in the vacuum chamber are represented in the fig.1. For direct measurements and in order to exclude deposited films sputtering, pyramidal traps are used. Four simple beryllium targets were placed in the thruster jet in order to obtain additional information and to confirm the results of investigations, represented in [2,3].

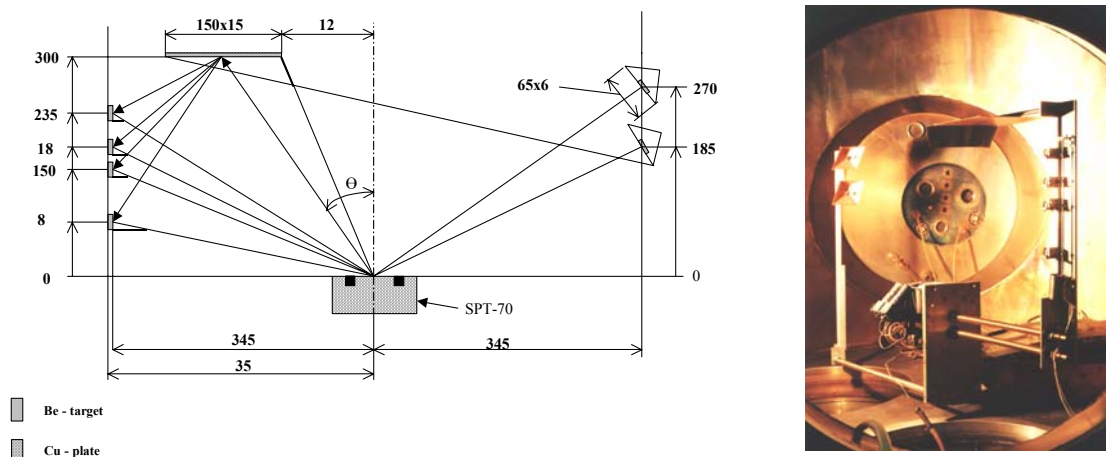


Figure 1: Scheme of the experiment and experimental unit in the vacuum chamber

The targets, placed inside the pyramids, are faced to their tops. Such disposition permits to exclude ion direct action onto forming films. Pyramid's walls are made of molybdenum. Admixture particles hit to the pyramid's surface, and then they are sputtered ones more by jet ions and come to the target. If the intensity of ion flow is sufficiently high, deposited film is sputtered completely and there is no any impurity particles accumulation on pyramid's surface. In this case integral flows of impurity particles at trap input and output will be the same. Of cause a few particles can be on the pyramid surface in dynamic equilibrium state. But if duration of the experiment is big enough, this phenomenon can be neglected. It is necessary to point out that impurity particles can be re-sputtered repeatedly and this fact permits to obtain more uniform distribution of impurity particles at trap output.

Such method was used in order to measure sputtered products flows and its composition (the SPT -70 isolator was made of AlB+BN, which operated for 70 hours). The experiment was carried out in the vacuum chamber with oil-free pumps. Two pyramids were placed under angles  $55^\circ$  and  $64^\circ$  relatively thruster's axis (according to [1-3] just under these angles the films of impurity particles are sputtered completely, so trap input flow will equal the flow coming to the target surface. Ion current density in the points of traps location was 0.08 and 0.05 mA/cm<sup>2</sup> respectively. The samples were exposed for 12 hours (3 runs 4 hours each). First 2 hours of operation the simple targets were protected from jet action and from the flows by special copper screen. It permitted to decrease film composition variation by the account of oxides sputtering from copper screen surface.

### Method of ion-beam investigation

The targets examination was carried out in the IPTM PAS ion-beam complex Sockol-3 by RBS method. RBS spectrums are recorded with standard double-detector scheme of measurement under  $E_0=1$  MeV. As far as there were lot light elements among deposited atoms, spectrum of scattering for He and H jointly were used. Also due to this reason polished Be plates 10 x 10 x 0.25 mm were used as a substrate. In all experiments B was a marker using which the total flow of impurity particles was estimated.

The main aim of film examination was to determine the total amount atoms of Cu and impurities, deposited on to the targets. RBS spectrums are processed with the help of approximate interactive software RUMP trying to obtain the best agreement between experimental spectrums for  $H^+$  and  $He^+$  for  $\vartheta_1=160^\circ$  and  $\vartheta_2=120^\circ$  and all theoretical spectrums, corresponding to single profile of concentration over film thickness.

The calculations showed that profiles for the films, deposited in pyramids (fig.2) are differ sufficiently from the profiles obtained at the non-protected targets (fig.3). Besides, it was found out that there were periodical variations of film composition over its thickness, correlating with the amount of thruster ignitions.

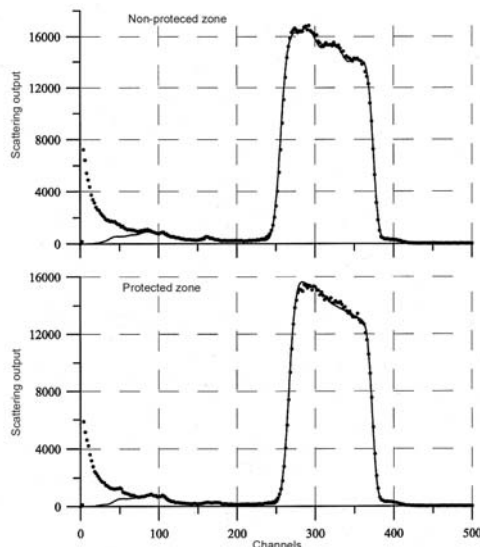


Figure 2: Theoretical and experimental RBS spectrums ( $He^+$ ,  $E=1$ MeV) for non-protected and protected parts of the target #4 ( $\gamma=56^\circ$ ). Protected part of the sample is characterized by film growth with great thickness. On the spectrum one can see sinuosity corresponding to thruster ignitions (3 stages 4 hours). Channel cost is 1.9 keV/channel; every second channel is shown

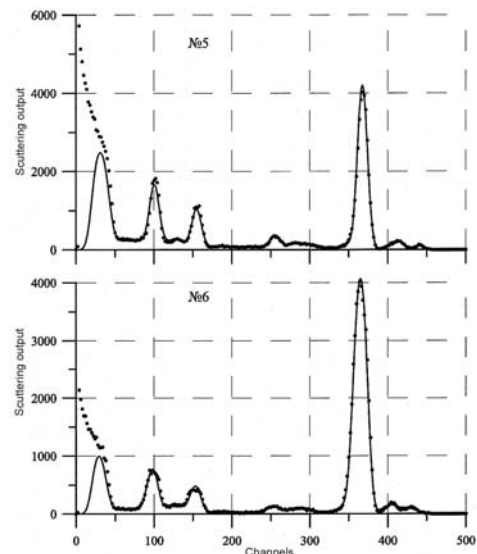


Figure 3: Theoretical and experimental RBS spectrums ( $He^+$ ,  $E=1$ MeV) for and protected the target N5 ( $\gamma=62^\circ$ ) and for the target #6( $\gamma=52^\circ$ ) placed inside the pyramidal traps. Targets have thinner films (respectively non-protected targets). Channel cost is 1.9 keV/channel; every second channel is shown

### Boron content in the films

Boron content in the films was determined according to nuclear resonance reaction  $^{11}\text{B}(p;\alpha)^8\text{B} \rightarrow 2\alpha$ . The energy of resonance is  $E_r=662$  keV, range  $\Delta E=300$  keV. The measurement were done under  $E_r=690$  keV with relative method. The initial ceramic tested with RBS method was used as a standard. Ceramic composition –  $\text{B}_{0.31}\text{N}_{0.38}\text{Al}_{0.06}(\Sigma x_i)_{0.25}$ . The main problem was to compare the sizes of the areas in which boron atoms were. The matter of fact that the ceramic may be imaged as a macro-volume with relatively uniform composition and so it is reasonable to assume that  $\alpha$ -particles birth is formed in the layer with  $\Delta_r=5\mu\text{m}$ . At the same time the thickness of the layer in which boron atoms are accumulated in the targets, is about  $0.1\mu\text{m}$ . So, analyzing films, it is necessary to introduce a correction factor close to 50. Nuclear spectrums normalization was done using RBS H<sup>+</sup> spectrums procession (spectrums were recorded with detector placed under angle of scattering  $\theta_1=1600$ ). Data about film composition, obtained with RBS and nuclear resonance reaction, is represented in the tables 1 and 2.

Table 1: The results of processing of the RBS spectrums, obtained for protected (●) and opened (○) parts of targets

Target	S	Layer		Composition, % at.												
		$\delta, \text{\AA}$	$N, \text{cm}^{-2}$	Cu	C	Al	O	N	B	Cl	S	Pt	Ca	Mo	Si	
#1 R=35.4 $\theta=76.9$	●	300	$2.7 \cdot 10^{+17}$	0.576	0.311	0.012	0.058	0.029		0.003	0.003	0.001	0.003	0.006	0.000	
		495	$4.4 \cdot 10^{+17}$	0.582	0.300	0.009	0.067	0.028		0.003	0.003	0.001	0.003	0.006	0.000	
		170	$1.5 \cdot 10^{+17}$	0.497	0.336	0.007	0.075	0.062		0.006	0.006	0.001	0.003	0.007	0.000	
	Σ	965	$9.38 \cdot 10^{+17}$	0.518	0.284	0.009	0.060	0.031	0.083	0.003	0.003	0.001	0.003	0.006	0.000	
	○	325	$2.9 \cdot 10^{+17}$	0.560	0.319	0.020	0.056	0.028		0.003	0.003	0.001	0.006	0.006	0.000	
		495	$4.4 \cdot 10^{+17}$	0.556	0.302	0.015	0.053	0.053		0.005	0.005	0.001	0.005	0.006	0.000	
		170	$1.5 \cdot 10^{+17}$	0.469	0.334	0.015	0.059	0.088		0.012	0.012	0.001	0.006	0.006	0.000	
	Σ	990	$9.51 \cdot 10^{+17}$	0.502	0.289	0.015	0.051	0.047	0.075	0.005	0.005	0.001	0.005	0.006	0.000	
	#2 R=37.6 $\theta=66.5$	●	650	$5.80 \cdot 10^{+17}$	0.562	0.230	0.023	0.110	0.046						0.005	0.023
			55	$5.00 \cdot 10^{+16}$	0.551	0.236	0.024	0.113	0.047						0.005	0.024
135			$1.35 \cdot 10^{+17}$	0.526	0.244	0.029	0.117	0.049						0.005	0.029	
350			$3.10 \cdot 10^{+17}$	0.590	0.211	0.025	0.101	0.042						0.005	0.025	
180			$1.6 \cdot 10^{+17}$	0.519	0.242	0.034	0.116	0.048						0.005	0.034	
340			$3.00 \cdot 10^{+17}$	0.567	0.218	0.031	0.105	0.044						0.005	0.031	
Σ		1710	$1.64 \cdot 10^{+18}$	0.526	0.212	0.025	0.102	0.042	0.037					0.005	0.027	
○		720	$6.40 \cdot 10^{+17}$	0.573	0.286	0.010	0.063	0.052						0.006	0.010	
		190	$1.70 \cdot 10^{+17}$	0.549	0.302	0.010	0.066	0.055						0.006	0.010	
		200	$1.80 \cdot 10^{+17}$	0.594	0.272	0.009	0.059	0.050						0.005	0.009	
	505	$4.50 \cdot 10^{+17}$	0.561	0.294	0.010	0.064	0.053						0.006	0.010		
Σ	1615	$1.50 \cdot 10^{+18}$	0.545	0.277	0.010	0.060	0.050	0.033					0.006	0.010		
#3 R=39.1 $\theta=61.8$	●	495	$4.40 \cdot 10^{+17}$	0.541	0.246	0.017	0.098	0.074						0.005	0.017	
		350	$3.10 \cdot 10^{+17}$	0.582	0.224	0.016	0.090	0.067						0.005	0.016	
		90	$8.00 \cdot 10^{+16}$	0.541	0.246	0.017	0.098	0.074						0.005	0.017	
		145	$1.30 \cdot 10^{+17}$	0.518	0.259	0.018	0.104	0.078						0.006	0.018	
		460	$4.10 \cdot 10^{+17}$	0.582	0.224	0.016	0.090	0.067						0.005	0.016	
		180	$1.60 \cdot 10^{+17}$	0.518	0.259	0.018	0.104	0.078						0.006	0.018	
	Σ	2235	$2.09 \cdot 10^{+18}$	0.521	0.231	0.016	0.093	0.069	0.035					0.005	0.017	
	○	865	$7.70 \cdot 10^{+17}$	0.594	0.270	0.011	0.054	0.054						0.006	0.011	
		1110	$9.90 \cdot 10^{+17}$	0.571	0.285	0.011	0.057	0.057						0.006	0.011	
		Σ	1975	$1.84 \cdot 10^{+18}$	0.556	0.267	0.011	0.053	0.053	0.032				0.006	0.011	
Σ		1975	$1.84 \cdot 10^{+18}$	0.556	0.267	0.011	0.053	0.053	0.032				0.006	0.011		
#4 R=41.7 $\theta=55.7$	●	565	$5.05 \cdot 10^{+17}$	0.500	0.272	0.020	0.114	0.068						0.005	0.020	
		225	$2.00 \cdot 10^{+17}$	0.541	0.250	0.019	0.104	0.062						0.005	0.019	
		275	$2.45 \cdot 10^{+17}$	0.500	0.272	0.020	0.114	0.068						0.005	0.020	
		235	$2.10 \cdot 10^{+17}$	0.476	0.285	0.021	0.119	0.071						0.005	0.021	
		460	$4.10 \cdot 10^{+17}$	0.541	0.250	0.019	0.104	0.062						0.005	0.019	
		235	$2.10 \cdot 10^{+17}$	0.476	0.285	0.021	0.119	0.071						0.005	0.021	
	Σ	2510	$2.35 \cdot 10^{+18}$	0.491	0.252	0.019	0.105	0.063	0.032					0.005	0.020	
	○	315	$2.80 \cdot 10^{+17}$	0.563	0.258	0.056	0.070	0.047						0.005	0.000	
		675	$6.00 \cdot 10^{+17}$	0.586	0.255	0.015	0.076	0.051						0.006	0.010	
		955	$8.50 \cdot 10^{+17}$	0.582	0.267	0.015	0.073	0.048						0.005	0.010	
Σ		1945	$1.78 \cdot 10^{+18}$	0.565	0.255	0.021	0.072	0.048	0.017					0.005	0.008	

Table 2: The results of processing of the RBS spectrums, obtained for the targets inside pyramidal traps

Target	Layer		Composition, % at.												
	$\delta, \text{\AA}$	$N, \text{cm}^{-2}$	Cu	C	Al	O	N	S	Si	Mo	Cl	Sn	Tb	Ti	B
#5 R=39.2 $\theta=62$	250	$3.05 \cdot 10^{+17}$	0.071	0.304	0.012	0.212	0.028	0.006	0.014	0.006	0.001	0.003	0.000	0.043	0.299
#6 R=43.8 $\theta=52$	470	$4.92 \cdot 10^{+17}$	0.131	0.401	0.011	0.149	0.056	0.007	0.010	0.008	0.001	0.003	0.003	0.018	0.201

In order to decrease a share of the protons scattered by the target, the detector recording  $\alpha$ -particles was covered with MAILAR film with the thickness  $6 \mu\text{m}$ . The detector was placed under the angle  $\theta_2 = 120^\circ$  relatively the initial beam and was characterized by great output window  $\Omega = 5 \cdot 10^{-5} \pi$ . Energy losses of  $\alpha$ -particles in MAILAR are about  $\Delta E \approx 0.9 \text{ MeV}$ .

### Boron particles distribution in the jet

Boron particles distribution in the jet was determined according to boron quantity deposited onto the target during the experiment. It was assumed that all boron was deposited to the targets.

The relation between B flows at the pyramid input ( $nv_{in}$ ) and on the substrate ( $nv_{out}$ ) was determined numerically assuming that B was sputtered completely on the pyramid's walls and that sputtered particles were scattered over diffusion low. The results of calculation for impurity particles output flows for one of the traps is represented in the fig.4. The calculations are carried out with the help of the software [4], which permits to take into account energetic spectrum of jet ions and sputtered coefficient dependence on ion energy and incidental angle. The calculations permitted to find out that  $nv_{in}/nv_{out} = 0.97$ .

Experimental data procession was done according to the method described in details in [2,3]. B flows in the pyramids was calculated by simple division of deposited B amount to time of the experiment. The results of procession are represented in the fig.5. From this drawing one can see that there is good agreement between B flows

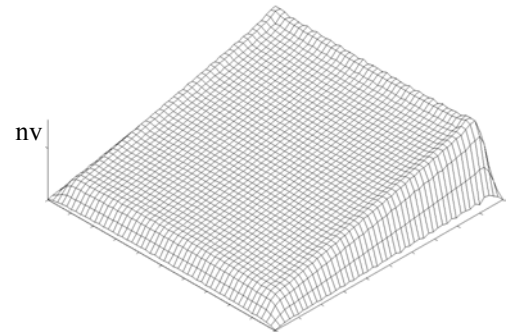


Figure 4: The diagram of sputtered particles flow density at the trap output

obtained by two methods. Particle flow density inclination is decreased and this phenomenon can be explained by the fact that collecting area of the pyramid is great, so flow is averaged over scattering angles.

Angled distribution of B particles in the SPT jet at the distance of 50 cm from thruster's cut

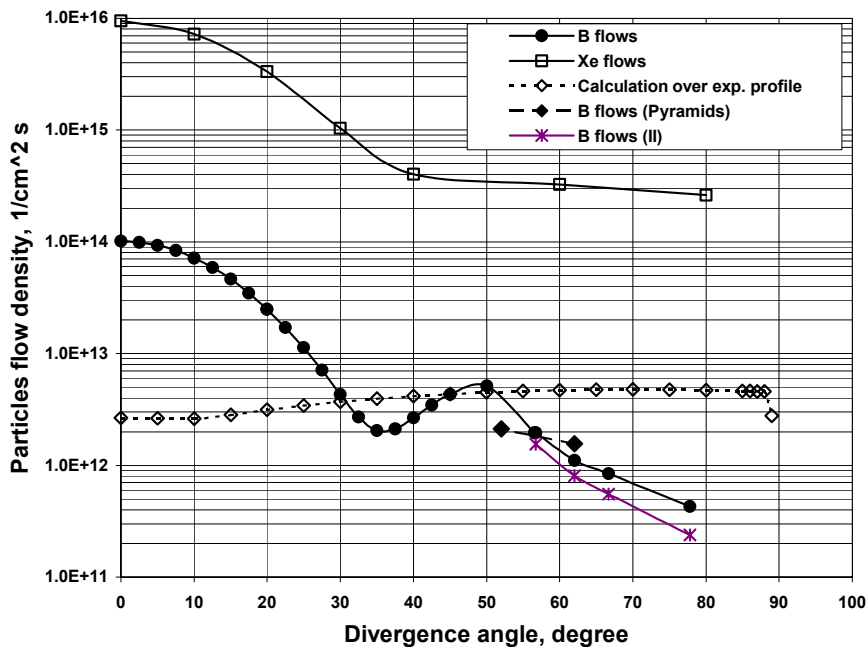


Figure 5.

### Conclusions

The information about sputtered particles angular distribution in the SPT M-70 jet was obtained. Characteristic values of the particle flows are  $1 - 2 \cdot 10^{12} / \text{cm}^2 \text{ s}$ . In general the results of the experiments

showed that pyramidal traps usage permits to obtain information about sputtered particles flows in the peripheral zones of the jet, where sputtering processes dominate over deposition processes.

## References

1. Pencil, E., Randolph, T., Manzella, D., "Far-Field Plume Contamination and Sputtering of the Stationary Plasma Thruster", AIAA-94-2855, 30<sup>th</sup> Joint Propulsion Conference, Indianapolis, Indiana, 1994.
2. Khartov S.A., Nadiradze A.B., Zikeeva Yu.V. Spacecraft Contamination by Sputtered Products of the SPT Ceramic Isolator // Proc. 3<sup>rd</sup> International Conference on Spacecraft Propulsion. Cannes, 10-13 October 2000, ESA SP-465, December 2000, pp.639-643.
3. Arbatsky V.M., Nadiradze A.B., Chirov A.A., Shaposhnikov V.V. Angled distribution of admixed elemental composition in the ERT jet with ion-beam method – "The Surface", No5, 2000 (in Russian).
4. Perrin V., Metois P., Khartov S., Nadiradze A. Simulation tools for the plasma propulsion and satellite environment // 52nd International Astronautical Congress Toulouse, France, October 1-5, 2001.